



Publication Year	2015
Acceptance in OA	2020-03-28T13:59:04Z
Title	CMB and BAO constraints for an induced gravity dark energy model with a quartic potential
Authors	Umiltà, C., Ballardini, M., FINELLI, FABIO, PAOLETTI, DANIELA
Publisher's version (DOI)	10.1088/1475-7516/2015/08/017
Handle	http://hdl.handle.net/20.500.12386/23665
Journal	JOURNAL OF COSMOLOGY AND ASTROPARTICLE PHYSICS
Volume	2015

CMB and BAO constraints for an induced gravity dark energy model with a quartic potential

C. Umiltà^{a,b,c} M. Ballardini^{d,e,f} F. Finelli^{e,f} and D. Paoletti^{e,f}

^aInstitut d'Astrophysique de Paris, CNRS (UMR7095), 98 bis Boulevard Arago, F-75014, Paris, France

^bUPMC Univ Paris 06, UMR7095, 98 bis Boulevard Arago, F-75014, Paris, France

^cSorbonne Universités, Institut Lagrange de Paris (ILP), 98 bis Boulevard Arago, 75014 Paris, France

^dDIFA, Dipartimento di Fisica e Astronomia, Via Bertini Pichat, I-40129 Bologna, Italy

^eINAF-IASF Bologna, via Gobetti 101, I-40129 Bologna, Italy

^fINFN, Sezione di Bologna, Via Irnerio 46, I-40126 Bologna, Italy

E-mail: umilta@iap.fr, ballardini@iasfbo.inaf.it, finelli@iasfbo.inaf.it, paoletti@iasfbo.inaf.it

Abstract. We study the predictions for structure formation in an induced gravity dark energy model with a quartic potential. By developing a dedicated Einstein-Boltzmann code, we study self-consistently the dynamics of homogeneous cosmology and of linear perturbations without using any parametrization. By evolving linear perturbations with initial conditions in the radiation era, we accurately recover the quasi-static analytic approximation in the matter dominated era. We use PLANCK 2013 data and a compilation of baryonic acoustic oscillation (BAO) data to constrain the coupling γ to the Ricci curvature and the other cosmological parameters. By connecting the gravitational constant in the Einstein equation to the one measured in a Cavendish-like experiment, we find $\gamma < 0.0012$ at 95% CL with PLANCK 2013 and BAO data. This is the tightest cosmological constraint on γ and on the corresponding derived post-Newtonian parameters. Because of a degeneracy between γ and the Hubble constant H_0 , we show how larger values for γ are allowed, but not preferred at a significant statistical level, when local measurements of H_0 are combined in the analysis with PLANCK 2013 data.

Contents

1	Introduction	1
2	Dark Energy within Induced Gravity	2
3	The evolution of cosmological fluctuations	3
4	CMB anisotropies and Matter Power spectrum	5
5	Constraints from cosmological observations	6
5.1	Combination with local measurements	9
6	Conclusions	10

1 Introduction

Inflation or quintessence are naturally embedded in scalar-tensor theories of gravity. In these models the scalar field which regulates the gravitational coupling also drives the acceleration of the Universe. The non-minimal coupling to gravity can change significantly the perspective on inflation or quintessence in Einstein general relativity. In the inflationary context, for instance, a large coupling of the inflaton to gravity allows potentials with a self-coupling which would be excluded in the minimally coupled case [1–4]. In the dark energy context, for example the coupling to gravity could allow super-acceleration (i.e., $\dot{H} > 0$) with standard kinetic terms for the scalar field [5].

In this paper we consider *induced gravity* (IG) with a quartic potential $V(\sigma) = \lambda\sigma^4/4$ as a simple scalar-tensor dark energy model:

$$S = \int d^4x \sqrt{-g} \left[\frac{\gamma\sigma^2 R}{2} - \frac{g^{\mu\nu}}{2} \partial_\mu \sigma \partial_\nu \sigma - \frac{\lambda}{4} \sigma^4 + \mathcal{L}_m \right]. \quad (1.1)$$

where \mathcal{L}_m denotes the contribution by matter and radiation. Under a simple field redefinition $\gamma\sigma^2 = \phi/(8\pi)$, the above action can be cast in a Brans-Dicke-like model [6] with a quadratic potential:

$$S = \int d^4x \sqrt{-g} \left[\frac{1}{16\pi} \left(\phi R - \frac{\omega_{\text{BD}}}{\phi} g^{\mu\nu} \partial_\mu \phi \partial_\nu \phi \right) - \frac{m^2}{2} \phi^2 + \mathcal{L}_m \right], \quad (1.2)$$

with the following relation between the dimensionless parameters of the two theories:

$$\omega_{\text{BD}} = \frac{1}{4\gamma} \quad m = \frac{\sqrt{2\lambda}}{16\pi\gamma}. \quad (1.3)$$

The action in Eq. (1.1), which contains only dimensionless parameters, was introduced to generate the gravitational constant and inflation by spontaneous breaking of scale invariance in absence of matter [7]. In the context of late cosmology, this action was studied in Refs. [8, 9] to reduce the time dependence of the effective gravitational constant in the original Brans-Dicke model (i.e., with a vanishing potential [6]) and to generate an effective cosmological constant. The cosmological background dynamics from Eq. (1.1) was shown to be consistent with observations for small γ , i.e., $\gamma \lesssim 10^{-2}$ [10].

The potential term in Eq. (1.1) is important for the global dynamics of the model and modifies the original Brans-Dicke attractor with power-law time dependence of the scalar field in presence of non-relativistic matter, i.e., $a(t) = (t/t_0)^{(2\omega_{\text{BD}}+2)/(3\omega_{\text{BD}}+4)}$ and $\Phi = \Phi_0(t/t_0)^{2/(3\omega_{\text{BD}}+4)}$. At recent times, the potential term drives the Universe into acceleration and Einstein gravity plus a cosmological constant with a time-independent value of the scalar field emerge as an attractor among homogeneous cosmologies for the model in Eq. (1.1).

In this paper we study structure formation in the IG dark energy with a quartic potential in Eq. (1.1). We study how gravitational instability at linear level depends on γ through a dedicated Einstein-Boltzmann code. We then use these theoretical predictions for cosmological observables to constrain the model with the PLANCK 2013 data [11–13], a compilation of baryonic acoustic oscillations (BAO) data [14–16] and local measurements of the Hubble constant [17–19].

2 Dark Energy within Induced Gravity

The Friedmann and the Klein-Gordon equations for IG in a flat Robertson-Walker metric are respectively:

$$H^2 + 2H\frac{\dot{\sigma}}{\sigma} = \frac{\sum_i \rho_i + V(\sigma)}{3\gamma\sigma^2} + \frac{\dot{\sigma}^2}{6\gamma\sigma^2} \quad (2.1)$$

$$\ddot{\sigma} + 3H\dot{\sigma} + \frac{\dot{\sigma}^2}{\sigma} + \frac{1}{(1+6\gamma)}\left(V_{,\sigma} - \frac{4V}{\sigma}\right) = \frac{1}{(1+6\gamma)}\frac{\sum_i(\rho_i - 3p_i)}{\sigma} \quad (2.2)$$

once the Einstein trace equation:

$$-\gamma\sigma^2 R = T - (1+6\gamma)\partial_\mu\sigma\partial^\mu\sigma - 4V - 6\gamma\sigma\Box\sigma \quad (2.3)$$

is used. In the above $V_{,\sigma}$ denotes the derivative of the potential $V(\sigma)$ with respect to σ , the index i runs over all fluid components, i.e. baryons, cold dark matter (CDM), photons and neutrinos, and we use a dot for the derivative with respect to the cosmic time. When considering $V \propto \sigma^4$ the potential cancels out from the Klein-Gordon equation and the scalar field is driven by non-relativistic matter. In the rest of the paper we will restrict ourselves to $V(\sigma) = \lambda\sigma^4/4$.

We consider the scalar field σ at rest deep in the radiation era, since an initial non-vanishing time derivative would be rapidly dissipated [10]. The scalar field is then driven by non-relativistic matter to an asymptotically value higher than the one it had in the radiation era as can be seen in the left panel of Fig. (1); when the scalar field freezes the Universe is driven in a de Sitter era by the scalar field potential which behaves as an effective cosmological constant [8, 10], as can be seen in the central panel of Fig. (1). Since σ regulates the gravitational strength in the Friedmann equations, the present value of the field σ_0 can be connected the gravitational constant G measured in laboratory Cavendish-type and solar system experiments by the relation:

$$\gamma\sigma_0^2 = \frac{1}{8\pi G} \frac{1+8\gamma}{1+6\gamma} \quad (2.4)$$

where $G = 6.67 \times 10^{-8} \text{ N cm}^3 \text{ g}^{-1} \text{ s}^{-2}$. The above equation assumes that σ is effectively massless on Solar System scales. Note that the scalar field σ is effectively massless in the radiation dominated era, as can be seen in Eq. (2.2).

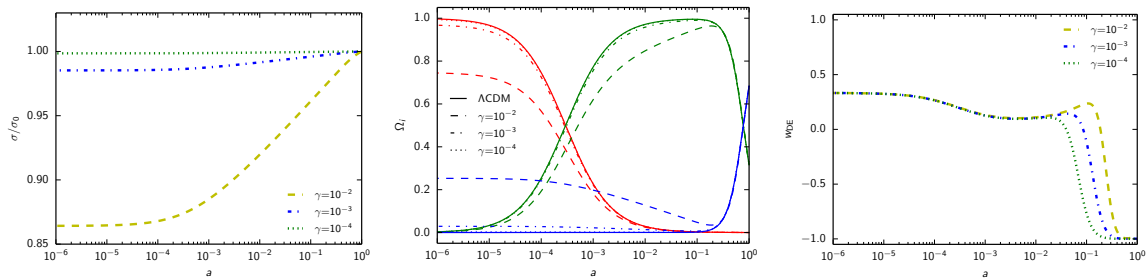


Figure 1. Evolution of σ/σ_0 (left panel), Ω_i (middle panel) and w_{DE} (right panel) as function of $\ln(a)$ for different choices of γ .

The evolution of the background cosmology can be easily compared with dark energy in Einstein gravity with a Newton's constant \tilde{G}_N given by the scalar field value at present $\tilde{G} = (8\pi\gamma\sigma_0)^{-1}$. The Friedmann equation can be therefore rewritten by introducing an effective dark energy component [20], whose energy and pressure densities for this model are [10]:

$$\begin{aligned}\rho_{\text{DE}} &= \frac{\sigma_0^2}{\sigma^2} \left(\frac{\dot{\sigma}}{2} - 6\gamma H \dot{\sigma} + \lambda \frac{\sigma^4}{4} \right) + \sum_i \rho_i \left(\frac{\sigma_0^2}{\sigma^2} - 1 \right) \\ p_{\text{DE}} &= \frac{\sigma_0^2}{\sigma^2} \left[\frac{\dot{\sigma}}{2} - 2\gamma H \dot{\sigma} - \lambda \frac{\sigma^4}{4} + \sum_i \frac{2\gamma\rho_i + p_i}{1 + 6\gamma} \right] - \sum_i p_i.\end{aligned}\quad (2.5a)$$

In the central panel of Fig. (1) we display the time evolution of the density contrasts of radiation - $\Omega_{\text{R}} \equiv (\rho_{\nu} + \rho_{\gamma}) / (3\gamma\sigma_0^2 H^2)$ -, matter - $\Omega_{\text{M}} \equiv (\rho_b + \rho_{\text{CDM}}) / (3\gamma\sigma_0^2 H^2)$ - and effective dark energy - $\Omega_{\text{DE}} \equiv \rho_{\text{DE}} / (3\gamma\sigma_0^2 H^2)$ -. As a third panel in Fig. (1), we display the time evolution of the parameter of state of the effective dark energy component, $w_{\text{DE}} \equiv p_{\text{DE}} / \rho_{\text{DE}}$.

3 The evolution of cosmological fluctuations

As for the background, we study linear fluctuations in the Jordan frame. We consider metric fluctuation in the longitudinal gauge:

$$ds^2 = -dt^2(1 + 2\Psi(t, \mathbf{x})) + a^2(t)(1 - 2\Phi(t, \mathbf{x}))dx^i dx_i \quad (3.1)$$

and for the scalar field:

$$\sigma(t, \mathbf{x}) = \sigma(t) + \delta\sigma(t, \mathbf{x}). \quad (3.2)$$

The perturbed Einstein equations for our IG model with a quartic potential in the longitudinal gauge are:

$$3H(\dot{\Phi} + H\Psi) + \frac{k^2}{a^2}\Phi + 3\frac{\dot{\sigma}}{\sigma}(\dot{\Phi} + 2H\Psi) - \frac{\dot{\sigma}^2}{2\gamma\sigma^2}\Psi = -\frac{1}{2\gamma\sigma^2}\left[3\dot{\sigma}\delta\dot{\sigma} - 6H^2\gamma\sigma\delta\sigma - 6H\gamma(\dot{\sigma}\delta\sigma + \sigma\dot{\delta}\sigma) - \frac{2\gamma k^2}{a^2}\delta\sigma + \sum_i\delta\rho_i + \lambda\sigma^3\delta\sigma\right], \quad (3.3a)$$

$$\dot{\Phi} + \Psi\left(H + \frac{\dot{\sigma}}{\sigma}\right) = \frac{a}{2k^2}\frac{\sum_i(\rho_i + p_i)\theta_i}{\gamma\sigma^2} + \frac{\delta\sigma}{\sigma}\left[\left(1 + \frac{1}{2\gamma}\right)\frac{\dot{\sigma}}{\sigma} - H\right] + \frac{\delta\dot{\sigma}}{\sigma}, \quad (3.3b)$$

$$\Phi - \Psi = \frac{2\delta\sigma}{\sigma} + \frac{3a^2}{2k^2}\frac{\sum_i(\rho_i + p_i)\bar{\sigma}_i}{\gamma\sigma^2}. \quad (3.3c)$$

In the above ρ_i, p_i ($\delta\rho_i, \delta p_i$) denote the energy and (longitudinal) pressure density perturbations for each matter component, respectively. The velocity potential and the anisotropic stress are denoted by θ_i and $\bar{\sigma}_i$. We refer to Ref. [21] for the conservation of the CDM, baryons, photons and neutrino energy-momentum tensors, since these equations are unchanged from those in Einstein gravity.

The Klein-Gordon equation at linear order in the longitudinal gauge is:

$$\begin{aligned} \delta\ddot{\sigma} + \delta\dot{\sigma}\left(3H + 2\frac{\dot{\sigma}}{\sigma}\right) + \left[\frac{k^2}{a^2} - \frac{\dot{\sigma}^2}{\sigma^2} + \frac{\sum_i(\rho_i - 3p_i)}{(1 + 6\gamma)\sigma^2}\right]\delta\sigma \\ = \frac{2\Psi\sum_i(\rho_i - 3p_i)}{(1 + 6\gamma)\sigma} + \frac{\sum_i(\delta\rho_i - 3\delta p_i)}{(1 + 6\gamma)\sigma} + \dot{\sigma}\left(3\dot{\Phi} + \dot{\Psi}\right). \end{aligned} \quad (3.4)$$

It is interesting to note that the equation for the field fluctuation does not depend on the potential explicitly for the self-interacting case, as for the background in Eq. (2.2).

We have modified the publicly available Einstein-Boltzmann code CLASS¹ [22, 23] to evolve background and linear fluctuations within induced gravity. Previous implementations of induced gravity in Einstein-Boltzmann codes include Refs. [24–28].

We initialize the fluctuation of the metric and of the matter components with adiabatic initial condition deep in the radiation era. We have tested our numerical results from our modified code against analytic approximations derived within the matter era. To this purpose we consider the quantity $\mu(k, a)$ which parametrize the deviations of Ψ from Einstein gravity [29, 30]. We consider the definition for $\mu(k, a)$ which holds also during the radiation dominated regime as in Ref. [31]:

$$k^2\Psi = -4\pi G a^2\mu(k, a)[\Delta + 3(\rho + p)\bar{\sigma}] \quad (3.5)$$

where $\Delta = \sum_i\delta\rho_i + 3aH(\rho_i + p_i)\theta_i/k^2$, with $\delta_i = \delta\rho_i/\rho_i$ and θ_i is the velocity potential. Analogously we consider the deviations from Einstein gravity of the difference between the Newtonian potentials, parametrized by δ , whose definition valid also in the radiation dominated regime is [31]:

$$k^2[\Phi - \delta(k, a)\Psi] = 12\pi G a^2\mu(k, a)(\rho + p)\bar{\sigma} \quad (3.6)$$

Our results are shown in Fig. (2). In the left panel we show the evolution of $\mu(k, a)$ for two wavenumbers ($k = 0.05, 0.005 \text{ Mpc}^{-1}$) and two values of the coupling to the Ricci

¹www.class-code.net

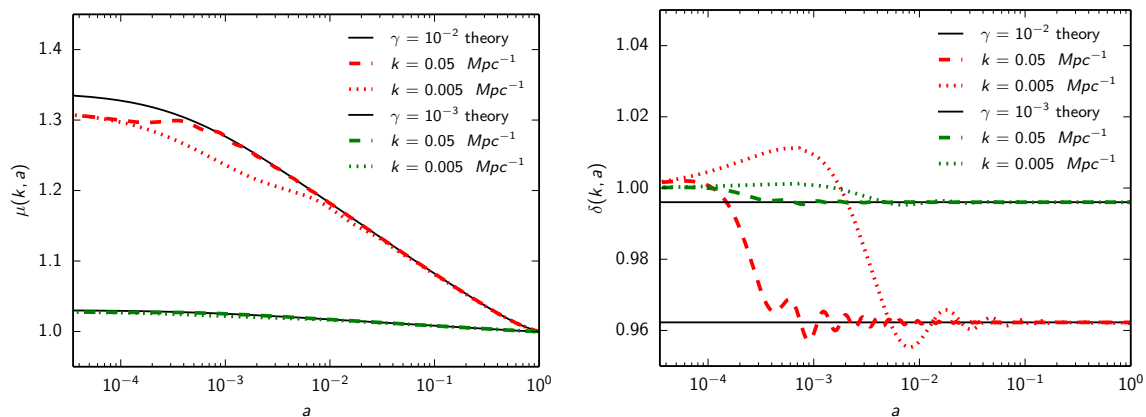


Figure 2. Comparison of theoretical approximations for μ and δ which parametrize deviations from Einstein gravity (black lines) with our numerical results for two wavenumbers ($k \text{ Mpc} = 0.05, 0.005$) and two values of the coupling to the Ricci curvature ($\gamma = 10^{-2}, 10^{-3}$).

curvature ($\gamma = 10^{-2}, 10^{-3}$). We compare our numerical results for $\mu(k, a)$ to the analytic approximation in the matter era:

$$\mu(k, a) = \frac{\sigma_0^2}{\sigma^2} \quad (3.7)$$

which is derived from Ref. [30] for our choice of the potential and for our identification of the gravitational constant in Eq. (2.4). Well after matter-radiation equivalence, the quasi-static analytic approximation for $k \gg aH$ in the matter era for $\mu(k, a)$ independent on k is well recovered. In the right panel of Fig. (2), we compare the evolution of $\delta(k, a)$ for the same two wavenumbers and two values of the coupling γ with the quasi-static approximation [5, 32, 33]:

$$\delta(k, a) = \frac{1 + 4\gamma}{1 + 8\gamma}. \quad (3.8)$$

Again, the analytic quasi-static approximation holds well after matter-radiation equality for sub-Hubble scales.

The agreement between our numerical treatment and the quasi-static approximation means that our self-consistent treatment of background and linear perturbations is sufficiently ready for precision cosmology. The two panels in Fig. (2) also show how the time evolution for μ and δ , independent on k , recovered within the quasi-static approximation is not valid when the wavelength is larger than the Hubble radius: predictions for CMB anisotropies in this model would be therefore affected by considering δ constant and equal to the value obtained within the quasi-static approximation at *all* times.

4 CMB anisotropies and Matter Power spectrum

In the left panel of Fig. (3) are shown the power spectra of the CMB temperature anisotropies for different values of γ ($10^{-2}, 10^{-3}, 10^{-4}$). The relative differences with respect to the Λ CDM reference model are shown in the right panel of Fig. (3). The change in the matter-radiation equality present in this scalar-tensor model [34] induces relative differences in the temperature power spectrum at few percent level for $\gamma = 10^{-3}$.

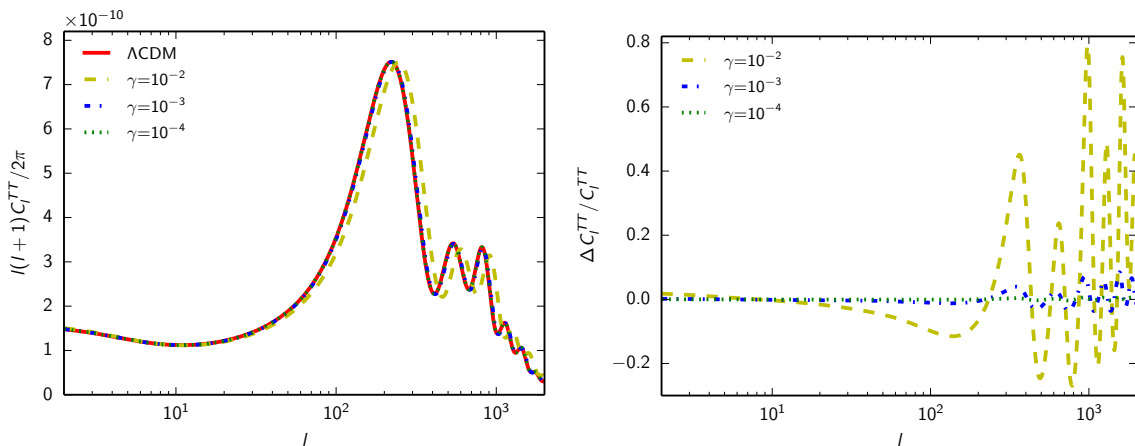


Figure 3. CMB temperature anisotropies power spectrum for different values of γ (left panel) and relative differences with respect to a reference ΛCDM (right panel).

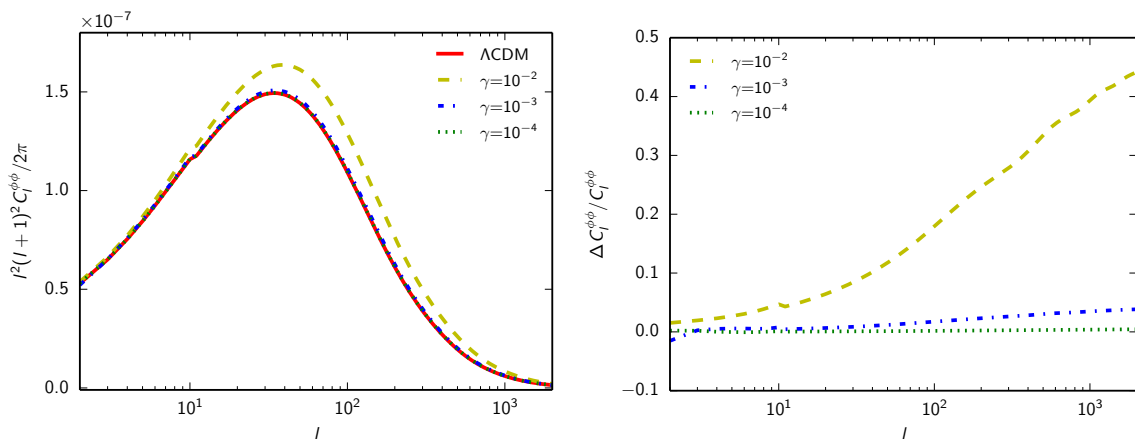


Figure 4. Lensing power spectrum for different values of γ (left panel) and relative differences with respect to a reference ΛCDM (right panel).

In Figs. (4, 5) we display the predictions for the spectrum of lensing potential and its correlation with the temperature field. In Fig. (6) we display the (linear) matter power spectrum at $z = 0$ and the relative differences with respect to the ΛCDM reference model. Overall, differences at the percent level are obtained for $\gamma = 10^{-3}$ in different cosmological observables.

5 Constraints from cosmological observations

We explore the parameter space by the Monte Carlo code for Cosmological Parameter extraction MONTE PYTHON² [35] connected to the modified version of the Einstein-Boltzmann code CLASS used in the previous sections. We use the nominal mission data release from PLANCK, available from the Planck Legacy Archive³ [11]. The PLANCK likelihood covering

²www.montepython.net

³pla.esac.esa.int/pla/aio/planckProducts.html

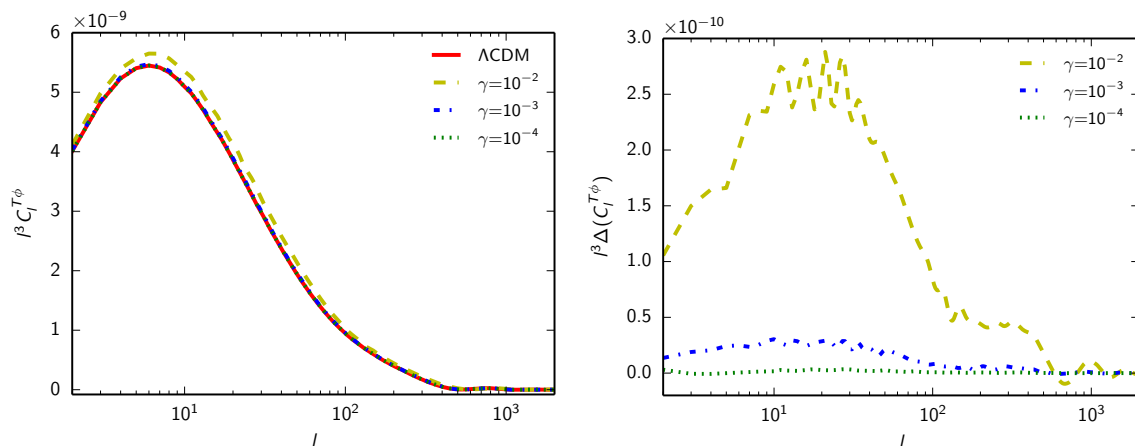


Figure 5. Temperature-lensing cross-correlation power spectrum for different values of γ (left panel) and differences with respect to a reference Λ CDM (right panel).

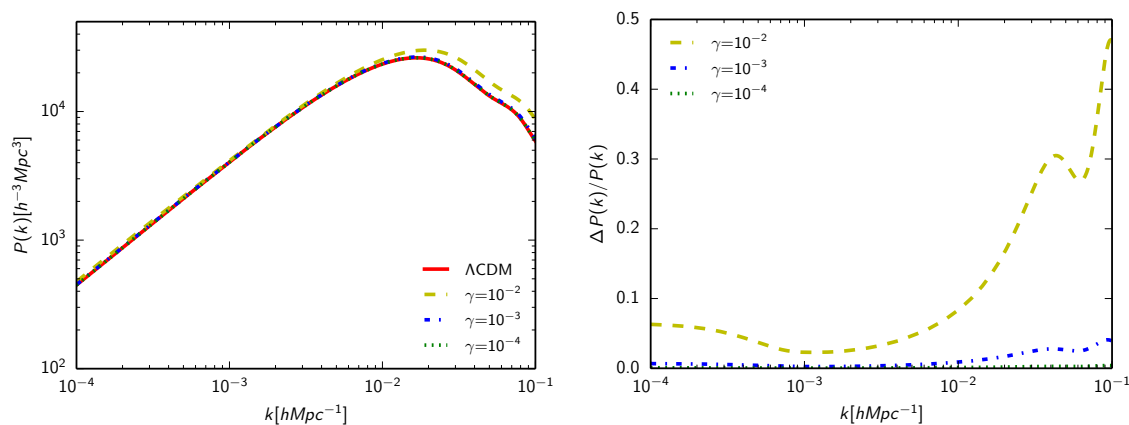


Figure 6. Linear matter power spectrum (at $z = 0$) for different values of γ (left panel) and relative differences with respect to a reference Λ CDM (right panel).

temperature anisotropies from $\ell = 2$ to 2500 is combined with the low- ℓ WMAP polarization data [36–38] (this combination is denoted as PLANCK 2013 in the following).

We use the PLANCK 2013 likelihood in combination with constraints on $D_V(\bar{z})/r_s$ (the ratio between the spherically averaged distance scale D_V to the effective survey redshift, \bar{z} , and the sound horizon, r_s) inferred from a compilation of BAO data. These are 6dFGRS data [14] at $\bar{z} = 0.106$, the SDSS-MGS data [15] at $\bar{z} = 0.15$, and the SDSS-DR11 CMASS and LOWZ data [16] at redshifts $\bar{z} = 0.57$ and 0.32 .

We vary the parameters of the flat Λ CDM model, i.e. the baryon density ($\Omega_b h^2$), the CDM density (Ω_{CDM}), the reduced Hubble parameter ($h = H_0/(100 \text{ km s}^{-1} \text{Mpc}^{-1})$), the reionization optical depth τ , the amplitude and tilt of the primordial spectrum of curvature perturbations (A_s and n_s) at the pivot scale $k_* = 0.05 \text{ Mpc}^{-1}$. The IG dark energy model with quartic potential is described by these six plus *one extra* parameter which quantifies the

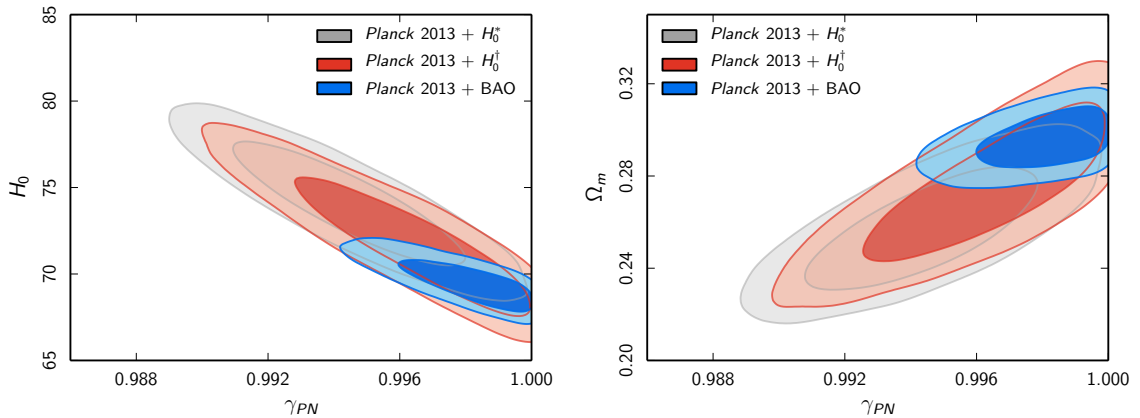


Figure 7. Comparison of marginalized joint 68% and 95% CL for (γ_{PN}, H_0) (left panel) and (γ_{PN}, Ω_m) (right panel) for PLANCK 2013 + H_0^* (grey contours), PLANCK 2013 + H_0^\dagger (red contours) and PLANCK 2013 + BAO (blue contours).

coupling to the Ricci curvature⁴. Following Ref. [39] we sample on the quantity ζ , defined as:

$$\zeta \equiv \ln(1 + 4\gamma) = \ln\left(1 + \frac{1}{\omega_{BD}}\right) \quad (5.1)$$

with the prior $[0, 0.039]$ used in Ref. [39]. In this paper we consider three massless neutrinos⁵. Nuisance parameters for foreground, calibration and beam uncertainties [11, 13].

Our results with PLANCK 2013 + BAO data for the main and derived parameters are summarized and compared with the Λ CDM values in Table 1. The induced gravity model with a quartic potential is not preferred over Einstein gravity with Λ ($\Delta\chi^2 \simeq -2\ln\mathcal{L} = 0.7$).

We quote the following PLANCK 2013 + BAO 95% CL constraint on the coupling to the Ricci curvature:

$$\gamma < 0.0012 \text{ (95 \% CL, PLANCK 2013 + BAO)}. \quad (5.2)$$

We quote as a derived parameter the corresponding constraint on the post-Newtonian parameter $\gamma_{PN} = (1 + 4\gamma)/(1 + 8\gamma)$ ⁶:

$$0.9953 < \gamma_{PN} < 1 \text{ (95 \% CL, PLANCK 2013 + BAO)}. \quad (5.3)$$

It is also useful to quote the derived constraints on the change of the Newton constant between the radiation era and the present time $\delta G_N/G_N \equiv (\sigma_i^2 - \sigma_0^2)/\sigma_0^2$:

$$\frac{\delta G_N}{G_N} = -0.015_{-0.006}^{+0.013} \text{ (95 \% CL, PLANCK 2013 + BAO)} \quad (5.4)$$

⁴The parameter of the Lagrangian λ and the initial value of the scalar field σ_i deep inside the radiation era are chosen to reproduce the present value of h and of the field in Eq. (2.4) by evolving the Friedmann and Klein-Gordon background equations.

⁵Note that the PLANCK collaboration assumes one massive neutrinos with a mass of 0.06 eV [13]. Given the interest in neutrino masses within modified gravity (see for example [40]), we will study this issue in the context of induced gravity in a separate publication. Even if the assumption of a mass of 0.06 eV has a small effect on the cosmological parameters at the PLANCK precision (as a 0.5σ shift to smaller value for H_0 [13]), we quote the results for a Λ CDM cosmology with three massless neutrinos in the following for a consistent comparison with the class of dark energy models studied here.

⁶In this class of models $\beta_{PN} = 1$.

	PLANCK 2013 + BAO Λ CDM	PLANCK 2013 + BAO
$10^5 \Omega_b h^2$	2215^{+24}_{-25}	2203 ± 25
$10^4 \Omega_c h^2$	1187^{+13}_{-14}	1207^{+18}_{-22}
H_0 [km s $^{-1}$ Mpc $^{-1}$]	$68.4^{+0.6}_{-0.7}$	$69.5^{+0.9}_{-1.2}$
τ	$0.091^{+0.012}_{-0.014}$	$0.088^{+0.012}_{-0.013}$
$\ln(10^{10} A_s)$	$3.089^{+0.024}_{-0.027}$	$3.090^{+0.024}_{-0.026}$
n_s	0.9626 ± 0.0053	0.9611 ± 0.0053
ζ	...	< 0.0047 (95% CL)
$10^3 \gamma$...	< 1.2 (95% CL)
γ_{PN}	...	> 0.9953 (95% CL)
Ω_m	0.301 ± 0.008	0.295 ± 0.009
$\delta G_N / G_N$...	$-0.015^{+0.013}_{-0.006}$
$10^{13} \dot{G}_N(z=0) / G_N$ [yr $^{-1}$]	...	$-0.61^{+0.55}_{-0.25}$
$10^{23} \ddot{G}_N(z=0) / G_N$ [yr $^{-2}$]	...	$0.86^{+0.33}_{-0.78}$

Table 1. Constraints on main and derived parameters (at 68% CL if not otherwise stated).

and the constraint on its derivative ($\dot{G}_N / G_N \equiv -2\dot{\sigma}_0 / \sigma_0$) at present time:

$$\frac{\dot{G}_N}{G_N}(z=0) = -0.61^{+0.55}_{-0.25} [\times 10^{-13} \text{ yr}^{-1}], \text{ (95\% CL, PLANCK 2013 + BAO)}. \quad (5.5)$$

The constraints derived here are tighter than those obtained in the literature with PLANCK 2013 data for similar scalar-tensor models with a power-law potential [39, 41] (see Refs. [42–44] for analysis with pre-PLANCK data). Avilez and Skordis [41] considered the case of a constant potential in Brans-Dicke-like theory and quote $(1 + 6\gamma)/(1 + 8\gamma) = 1.07^{+0.11}_{-0.10}$ at 95% CL as the tightest constraint with a prior $\omega_{\text{BD}} > -3/2$; we obtain $[0.998, 1]$ as the 95% CL range for the same quantity with PLANCK 2013 + BAO by varying ζ in the interval $[0, 0.039]$. Li et al. [39] considered the case of a linear potential in Brans-Dicke (i.e., a quadratic potential in induced gravity) and quote $0 < \zeta < 0.549 \times 10^{-2}$ at 95% CL and $\dot{G}_N / G_N = -1.42^{+2.48}_{-2.27}$ at 68% CL from PLANCK 2013 with the same prior on ζ , although in combination with a different compilation of BAO data [39]. Note that for power-law potentials different from the quartic case studied here, Einstein gravity plus a cosmological constant with σ independent on time is not the attractor at future times [45]. We therefore expect that the models studied in Refs. [39, 41] differ from the case of a quartic potential, in particular at recent redshifts.

5.1 Combination with local measurements

As from Table 1, the model considered here prefers a higher value of the Hubble parameter H_0 with respect to Λ CDM. We therefore analyze the combination of the local measurements of the Hubble constant with PLANCK 2013 and BAO data. The local estimates of H_0 are consistently higher than those from CMB (and BAO) and this discrepancy became a 2.5 σ tension after the PLANCK 2013 release [13]. This tension might be sign of new physics, although reanalysis subsequent to the PLANCK 2013 release have highlighted how hidden systematics and underestimated uncertainties could hide in the local measurements of H_0 [18, 19]. For these reasons we consider separately the impact of two different local estimates of H_0 , such as $H_0 = 73.8 \pm 2.4$ km s $^{-1}$ Mpc $^{-1}$ [17], denoted as H_0^* , and $H_0 = 70.6 \pm 3.0$ km s $^{-1}$ Mpc $^{-1}$ [19], denoted as H_0^\dagger . Our results are summarized in Table 2 and Fig. (7).

	PLANCK 2013 + H_0^*	PLANCK 2013 + H_0^\dagger	PLANCK 2013 + BAO + H_0^\dagger
$10^5 \Omega_b h^2$	2219 ± 28	2213^{+28}_{-29}	2203 ± 26
$10^4 \Omega_c h^2$	1188^{+25}_{-26}	1194^{+25}_{-25}	1207^{+18}_{-22}
H_0 (km s $^{-1}$ Mpc $^{-1}$)	$74.1^{+2.3}_{-2.4}$	$72.1^{+2.2}_{-3.1}$	$69.64^{+0.88}_{-1.11}$
τ	$0.092^{+0.013}_{-0.014}$	$0.091^{+0.013}_{-0.015}$	$0.088^{+0.012}_{-0.014}$
$\ln(10^{10} A_s)$	$3.098^{+0.025}_{-0.027}$	$3.095^{+0.025}_{-0.028}$	$3.091^{+0.024}_{-0.027}$
n_s	$0.9704^{+0.0070}_{-0.0072}$	$0.9667^{+0.0075}_{-0.0078}$	$0.9613^{+0.0055}_{-0.0054}$
ζ	0.0056 ± 0.0023	< 0.0083 (95% CL)	0.0047 (95% CL)
$10^3 \gamma$	1.4 ± 0.6	< 2.1 (95% CL)	< 1.2 (95% CL)
γ_{PN}	$0.9944^{+0.0023}_{-0.0022}$	> 0.9918 (95% CL)	> 0.9954 (95% CL)
Ω_m	$0.257^{+0.016}_{-0.019}$	$0.274^{+0.022}_{-0.021}$	$0.294^{+0.009}_{-0.008}$
$\delta G_N / G_N$	$-0.041^{+0.017}_{-0.016}$	-0.028 ± 0.012	$-0.016^{+0.010}_{-0.006}$
$10^{13} \dot{G}_N(z=0) / G_N$ [yr $^{-1}$]	$-1.56^{+0.61}_{-0.58}$	$-1.10^{+0.83}_{-0.49}$	$-0.64^{+0.52}_{-0.25}$
$10^{23} \ddot{G}_N(z=0) / G_N$ [yr $^{-2}$]	$2.4^{+0.9}_{-1.0}$	$1.7^{+0.7}_{-1.5}$	$0.89^{+0.24}_{-0.75}$

Table 2. Constraints on main and derived parameters at 68% CL (if not otherwise stated).

With the higher local estimate of H_0^* [17] we obtain a posterior on ζ which is different at 2σ level from Einstein gravity. With the lower estimate for H_0 obtained by Efstathiou [19] with the new revised geometric maser distance to NGC 4258 [18], we obtain a posterior probability for ζ compatible with Einstein gravity. As can be seen by comparing the last columns of Table 1 and 2, the lower local estimate of H_0^\dagger has almost a negligible impact when PLANCK 2013 and BAO data are combined.

6 Conclusions

We have studied structure formation in a induced gravity dark energy model with a quartic potential. In this model the current acceleration stage of the Universe and an accompanying change in the gravitational constant on large scales are due to a change in the background scalar field triggered by the onset of the matter dominated stage [8, 10].

We have shown that the model approaches Einstein gravity plus a cosmological constant in the limit $\gamma \rightarrow 0$ *also* at linear level. We have shown how the quasi-static parametrization with μ and γ independent on k holds only well after matter-radiation equality for sub-Hubble scales.

We have derived CMB and BAO combined constraints on γ for the case of induced gravity with a quartic potential. By using PLANCK 2013 [12] and BAO [14–16] data we derive the 95%CL constraint $\gamma < 0.0012$, which is tighter than previous cosmological constraints on similar models [39, 41]. This cosmological constraint is compatible, but weaker than those within the Solar System [10] which can be derived by Cassini data [46]. Since there is a positive correlation between γ and H_0 , the combination of local measurements of H_0 [17, 19] allows larger values of γ , but not at statistical significant level. This analysis shows how a self-consistent variation of G from the radiation era to the present time can be tightly constrained from PLANCK 2013 and BAO data at the percent level. It will be interesting to see how PLANCK 2015 data [47] change these constraints [48].

Acknowledgements

We wish to thank Julien Lesgourgues, Thomas Tram and Benjamin Audren for many useful suggestions on the use of the CLASS code and MONTEPYTHON code. We wish to thank Massimo Rossi for careful checking of the equations for cosmological perturbations and Levon Pogosian for useful comments on the draft. This work has been done within the Labex ILP (reference ANR-10-LABX-63) part of the Idex SUPER, and received financial state aid managed by the Agence Nationale de la Recherche, as part of the programme Investissements d'avenir under the reference ANR-11-IDEX-0004-02. The support by the "ASI/INAF Agreement 2014-024-R.0 for the Planck LFI Activity of Phase E2" is acknowledged.

References

- [1] B. L. Spokoiny, Phys. Lett. B **147** (1984) 39.
- [2] F. Lucchin, S. Matarrese and M. D. Pollock, Phys. Lett. B **167** (1986) 163.
- [3] D. S. Salopek, J. R. Bond and J. M. Bardeen, Phys. Rev. D **40** (1989) 1753.
- [4] R. Fakir and W. G. Unruh, Phys. Rev. D **41** (1990) 1783.
- [5] B. Boisseau, G. Esposito-Farese, D. Polarski and A. A. Starobinsky, Phys. Rev. Lett. **85** (2000) 2236.
- [6] C. Brans and R. H. Dicke, Phys. Rev. **124** (1961) 925.
- [7] A. Zee, Phys. Rev. Lett. **44** (1980) 703.
- [8] F. Cooper and G. Venturi, Phys. Rev. D **24** (1981) 3338.
- [9] C. Wetterich, Nucl. Phys. B **302** (1988) 668.
- [10] F. Finelli, A. Tronconi and G. Venturi, Phys. Lett. B **659** (2008) 466.
- [11] P. A. R. Ade *et al.* [Planck Collaboration], Astron. Astrophys. **571** (2014) A1.
- [12] P. A. R. Ade *et al.* [Planck Collaboration], Astron. Astrophys. **571** (2014) A15.
- [13] P. A. R. Ade *et al.* [Planck Collaboration], Astron. Astrophys. **571** (2014) A16.
- [14] F. Beutler, C. Blake, M. Colless, D. H. Jones, L. Staveley-Smith, L. Campbell, Q. Parker and W. Saunders *et al.*, Mon. Not. Roy. Astron. Soc. **416** (2011) 3017.
- [15] A. J. Ross, L. Samushia, C. Howlett, W. J. Percival, A. Burden and M. Manera, Mon. Not. Roy. Astron. Soc. **449** (2015) 1, 835.
- [16] L. Anderson *et al.* [BOSS Collaboration], Mon. Not. Roy. Astron. Soc. **441** (2014) 1, 24.
- [17] A. G. Riess, L. Macri, S. Casertano, H. Lampeitl, H. C. Ferguson, A. V. Filippenko, S. W. Jha and W. Li *et al.*, Astrophys. J. **730** (2011) 119 [Astrophys. J. **732** (2011) 129].
- [18] E. M. L. Humphreys, M. J. Reid, J. M. Moran, L. J. Greenhill and A. L. Argon, Astrophys. J. **775** (2013) 13.
- [19] G. Efstathiou, Mon. Not. Roy. Astron. Soc. **440** (2014) 2, 1138.
- [20] R. Gannouji, D. Polarski, A. Ranquet and A. A. Starobinsky, JCAP **0609** (2006) 016.
- [21] C. P. Ma and E. Bertschinger, Astrophys. J. **455** (1995) 7.
- [22] J. Lesgourgues, arXiv:1104.2932 [astro-ph.IM].
- [23] D. Blas, J. Lesgourgues and T. Tram, JCAP **1107** (2011) 034.
- [24] X. l. Chen and M. Kamionkowski, Phys. Rev. D **60** (1999) 104036.

- [25] F. Perrotta, C. Baccigalupi and S. Matarrese, *Phys. Rev. D* **61** (1999) 023507.
- [26] A. Riazuelo and J. P. Uzan, *Phys. Rev. D* **66** (2002) 023525.
- [27] R. Nagata, T. Chiba and N. Sugiyama, *Phys. Rev. D* **66** (2002) 103510.
- [28] F. Wu, L. e. Qiang, X. Wang and X. Chen, *Phys. Rev. D* **82** (2010) 083002.
- [29] G. B. Zhao, L. Pogosian, A. Silvestri and J. Zylberberg, *Phys. Rev. D* **79** (2009) 083513.
- [30] G. B. Zhao, H. Li, E. V. Linder, K. Koyama, D. J. Bacon and X. Zhang, *Phys. Rev. D* **85** (2012) 123546.
- [31] A. Hojjati, L. Pogosian and G. B. Zhao, *JCAP* **1108** (2011) 005.
- [32] L. Amendola, M. Kunz and D. Sapone, *JCAP* **0804** (2008) 013.
- [33] S. Tsujikawa, *Phys. Rev. D* **76** (2007) 023514.
- [34] A. R. Liddle, A. Mazumdar and J. D. Barrow, *Phys. Rev. D* **58** (1998) 027302.
- [35] B. Audren, J. Lesgourgues, K. Benabed and S. Prunet, *JCAP* **1302** (2013) 001.
- [36] L. Page *et al.* [WMAP Collaboration], *Astrophys. J. Suppl.* **170** (2007) 335.
- [37] C. L. Bennett *et al.* [WMAP Collaboration], *Astrophys. J. Suppl.* **208** (2013) 20.
- [38] G. Hinshaw *et al.* [WMAP Collaboration], *Astrophys. J. Suppl.* **208** (2013) 19.
- [39] Y. C. Li, F. Q. Wu and X. Chen, *Phys. Rev. D* **88** (2013) 084053.
- [40] H. Motohashi, A. A. Starobinsky and J. Yokoyama, *Phys. Rev. Lett.* **110** (2013) 12, 121302.
- [41] A. Avilez and C. Skordis, *Phys. Rev. Lett.* **113** (2014) 011101.
- [42] R. Nagata, T. Chiba and N. Sugiyama, *Phys. Rev. D* **69** (2004) 083512.
- [43] V. Acquaviva, C. Baccigalupi, S. M. Leach, A. R. Liddle and F. Perrotta, *Phys. Rev. D* **71** (2005) 104025.
- [44] F. Wu and X. Chen, *Phys. Rev. D* **82** (2010) 083003.
- [45] A. Cerioni, F. Finelli, A. Tronconi and G. Venturi, *Phys. Lett. B* **681** (2009) 383.
- [46] B. Bertotti, L. Iess and P. Tortora, *Nature* **425** (2003) 374.
- [47] R. Adam *et al.* [Planck Collaboration], arXiv:1502.01582 [astro-ph.CO].
- [48] M. Ballardini *et al.*, in preparation (2015).